Direct tray and point efficiency measurements including weeping effects through a convenient addon for air/water simulators

Sara Marchini[a,b,c*], Vineet Vishwakarma[a,b], Markus Schubert[b,*], Elisabetta Brunazzi[c], Uwe Hampel[a,b]

[a]Chair of Imaging Techniques in Energy and Process Engineering, Technische Universität Dresden, 01062 Dresden, Germany

[b]Institute of Fluid Dynamics, Helmholtz-Zentrum Dresden-Rossendorf, Bautzner Landstraße 400, 01328 Dresden, Germany

[c]Department of Civil and Industrial Engineering, University of Pisa, Largo Lucio Lazzarino 2, 56126 Pisa, Italy

*Corresponding authors: s.marchini@tu-dresden.de (S. Marchini)

m.schubert@hzdr.de (M. Schubert)

Abstract

A direct approach for determining the tray and point efficiencies of an industrial-scale distillation tray is proposed. The stripping of isobutyl acetate from an aqueous solution with air was used, which is a manageable and non-hazardous method applicable for performance tests in large hydraulic column mockups. This work represents the first application of this system in the case of tray columns exemplified for a sieve tray. A column of 800 mm internal diameter was used for conducting the stripping experiments. The distribution of isobutyl acetate in the liquid phase on the tray was obtained via liquid sampling at several deck positions and UV-spectroscopy analysis. A definition for the liquid-side tray efficiency at weeping conditions is proposed together with an experimental approach for

determining tray and point efficiencies in such conditions. The derived efficiency data show a good agreement with the model predictions and correlations.

Keywords

tray efficiency, point efficiency, isobutyl acetate stripping, tray column, mockup revamp, weeping

1. Introduction

Distillation columns are known to be the biggest energy consumers and the largest single investments in the chemical industry. It has been estimated that about half of the existing distillation columns globally are equipped with trays today and likely in the future, too[1].

A thorough understanding of the mass-transfer phenomena on the trays requires hydrodynamic investigations as well as tray and point efficiency data. Hydrodynamic studies are usually conducted in air/water mockups that are, apart from large pumps and blowers, relatively easy to build and operate[1]. Most of the manufacturing suppliers and vendors of column internals, such as trays, packings, and liquid distributors, etc., operate mockup facilities for hydraulic performance tests using air and water as the working fluids[2]. However, the determination of tray and point efficiencies requires more complex physical systems, experimental setups (e.g., semi-industrial distillation facilities, mockups with gas conditioning, recirculation and treatment) and analytics (e.g., gas-liquid chromatography)[1].

The tray efficiencies are experimentally determined by sampling the liquid and gas entering and leaving the tray. The physical systems used in the literature for efficiency measurements on trays can be classified into four categories namely hydrocarbon distillation systems, gas stripping systems, gas absorption systems and air humidification systems. A list of systems pertaining to each category can be found in **Table 1**.

Table 1. Physical systems used for efficiency measurements (TE – tray efficiency, PE – point efficiency, CP –concentration profile) on tray decks (S – sieve, BC – bubble cap, V – valve).

System	Tray dimensions	Tray deck	TE	PE	CP	Reference
Hydrocarbons distillation systems						
Cyclohexane/n-heptane	Φ 1.2 m	S	x			[3]
	Φ 0.429 m	S	x	x		[4]
i-Butane/n-butane	Φ 1.2 m	S	x			[3]
n-Propanol/sec-butanol	Φ 1.8 m	S	x			[5]
	Φ 0.61 m	BC	x			[5]
Acetic acid/water	Φ 0.46 m	S, BC	x			[6]
	Φ 0.46 m	S	x			[7]
Methanol/water	Φ 0.98 m	BC, S, etc.	x			[8]
	0.59 m × 0.37 m	S	x	x	x	[9]
Ethylene glycol/water	Φ 0.429 m	S	x	x		[4]
Methanol/ethanol	Φ 0.61 m	S	x	x	x	[10]
n-Propanol/toluene	Φ 0.46 m	V, S	x			[11]
Benzene/n-propanol	Φ 0.46 m	V, S	x			[11]
Gas stripping systems						
Air/O_2-water-glycerol	0.9 m × 0.3 m	S	x			[12]
Air/O_2-water	Φ 0.6 m	BC	x			[13]
	0.91 m × 0.24 m	S	x	x	x	14]
	Φ 1.2 m	S			x	15]
	Φ 0.12 m	S	x	x		16]
Air/NH_3-water	1.22 m × 0.81 m	S,V	x			17]
	0.9 m × 0.076 m	S	x		x	18]
Gas absorption systems						
NH_3-air/water	0.305 m × 0.013 m	S	x	x		[19]
CO_2-air/water	Φ 0.8 m	S	x			[20]
	0.9 m × 0.3 m	S	x			[12]
	0.305 m × 0.013 m	S	x	x	x	[21]
SO_2-air/ aqueous buffer solution	0.305 m × 0.013 m	S	x	x		[19]
Air humidification systems						
Air/water	Φ 0.12 m	S	x	x		[16]
	0.76 m × 1.04 m	S	x	x	x	[22]
	Φ 0.46 m	S	x			[7]

The peculiarities and limitations of these system categories hindering efficiency measurements are:

- **Hydrocarbon distillation systems**. The main disadvantage of these systems is the requirement of an industrial or semi-industrial distillation facility (i.e., condenser, reboiler, column that can resist non-ambient conditions, and so forth). The substances used are inherently hazardous, whereas high temperature and pressure are mostly applied. However, they are advantageous for directly investigating industrially-relevant physical systems.

- **Gas stripping systems**. Such systems involve stripping of low soluble gas from water. Although no reboiler or condenser is needed, the initial gas dissolution in the liquid demands extended pipe lengths, static mixers or a stirred vessel. Mostly oxygen is used as the dissolved gas. However, the most severe limitation is that the system approaches equilibrium in about 10 seconds right after the liquid enters the column[13]. Beyond, no significant mass transfer can be measured rendering the system unsuitable for large trays and low liquid flow rates (i.e., for high liquid residence times). To address the limitation of lower liquid residence time, Thomas and Haq[12] proposed using 50% wt. glycol-water solution instead of water only, which causes higher liquid viscosity and lower mass-transfer coefficients. However, due to glycol addition, the initial dissolution of oxygen in the liquid becomes even more cumbersome and requires efficient diffusers. The stripping of ammonia from water solution is another system used in the literature. Since ammonia can be dissolved in higher concentrations in water[23], it is applicable for trays with higher liquid residence times. However, higher concentrations of hazardous ammonia in the exiting gas demand additional safety measures (e.g., gas treatment).

- **Gas absorption systems**. The most common absorption systems utilize CO_2, which can be used solely or mixed with air at low concentrations[12,21]. Air-NH_3 and air-SO_2 mixtures at low concentrations were also used earlier[19]. These systems allow higher liquid residence times on the tray compared to stripping systems and, thus, are applicable for large trays. However, these gases pose serious health and safety hazards, even more at higher gas flow rates. Even in the low-concentration studies mentioned previously, the concentration of the exiting gas exceeds the safety exposure limit, requiring gas recirculation or treatment systems.

- **Air humidification systems**. In these systems, the measurements are performed at the gas outlet using humidity sensors. Such systems require precise conditioning of the incoming air for warranting mass-transfer measurements on the trays.

Based on the above-mentioned review, the traditional systems used for efficiency studies on distillation trays have numerous operational and technical limitations and safety concerns, which prevents their application particularly for large column setups and for low liquid flow rates, (i.e., for high liquid residence times).

Table 1 also illustrates that only few studies provide an experimental investigation of the point efficiency on large-scale trays. Instead, it is common practice to measure the point efficiency experimentally using small-scale setups only (e.g., Oldershaw columns[24]) or to extrapolate its value from measured tray efficiencies using available models. Another approach is using theoretical models or experimental correlations for predicting the number of transfer units that can be related to the point efficiency. All these approaches present specific drawbacks that will be discussed in a later section and that can prevent their application for determining the point efficiency on industrial-scale trays.

In industrial practice, distillation columns are designed to operate at a weeping fraction of maximum 20%, which is still considered acceptable[25]. As a rule of thumb, a weeping fraction of 20% can cause a reduction in tray efficiency of approx. 10%[26]. Nevertheless, the majority of the efficiency studies (including all studies reported in **Table 1**) ignores or does not account for the effect of weeping. In order to account for weeping, few theoretical models have been developed considering both uniform (e.g., Lockett et al.[27]) and non-uniform (e.g., Banik[28]) weeping conditions at total, partial or negligible mixing conditions for both liquid and vapour. On the experimental side, weeping rate has been extensively measured in the literature (e.g., Banik[28,29]), but no experimental approach for determining tray and point efficiencies accounting for weeping could be found in the available literature.

The present work proposes the isobutyl acetate stripping with air as a direct approach for the simultaneous determination of tray and point efficiencies on large-scale distillation trays. The first

application of the proposed physical system on distillation trays is demonstrated in this work. An easy to build experimental setup allows extending the method to virtually all operating conditions and environments. The proposed approach is recommended as a simple add-on to already available cold flow air/water experimental mockups, since only minor modifications are needed for fast acquisition of the tray and point efficiency data for thorough tray performance assessment. In addition, a full set of definitions for tray and point efficiencies in weeping conditions is proposed. Experiments are performed at a weeping fraction of approx. 16% and the effect of weeping on the calculated value of tray and point efficiencies is assessed.

2. Revisiting the efficiency concepts

2.1 Tray efficiency

Among the existing definitions of tray efficiency, the one proposed by Murphree[30] is the most preferred in the common use[31] and thus, it has been applied in this work. The Murphree tray efficiency represents the extent of separation achieved on a real cross-flow tray with respect to an ideal stage. Using the nomenclature shown in **Figure 1a** (highlighted by the dashed line), the definition of vapour[1]-side tray efficiency is given as

$$E_{\mathrm{MV}} = \frac{\bar{y}_{\mathrm{n}} - \bar{y}_{\mathrm{n-1}}}{\bar{y}^{*}_{\mathrm{n,d}} - \bar{y}_{\mathrm{n-1}}}, \qquad (1)$$

where $\bar{y}_{\mathrm{n}}$ is the average composition of the vapour leaving the tray, $\bar{y}_{\mathrm{n-1}}$ is the composition of the inlet vapour (assumed perfectly mixed), and $\bar{y}^{*}_{\mathrm{n,d}}$ is the vapour composition that is in equilibrium with the average composition of the liquid leaving the tray via the downcomer ($\bar{x}_{\mathrm{n,d}}$). The liquid-side tray efficiency is defined in analogy as

$$E_{\mathrm{ML}} = \frac{\bar{x}_{\mathrm{n+1,d}} - \bar{x}_{\mathrm{n,d}}}{\bar{x}_{\mathrm{n+1,d}} - \bar{x}^{*}_{\mathrm{n}}}, \qquad (2)$$

[1] The terms 'gas' and 'vapour' are used interchangeably in this work.

where $\bar{x}_n^*$ is the liquid composition in equilibrium with the average composition of the vapour leaving the tray.

Assuming that the vapour-liquid equilibrium data can be approximated by a line of slope m and intercept b and that the gas and liquid molar flow rates are constant, the liquid-side and vapour-side tray efficiencies can be related via material balance on the tray as

$$E_{\mathrm{MV}} = \frac{E_{\mathrm{ML}}}{E_{\mathrm{ML}} + \lambda(1 - E_{\mathrm{ML}})}\,, \tag{3}$$

where $\lambda = m\frac{G}{L}$, and G and L are the molar gas and liquid flow rates, respectively.

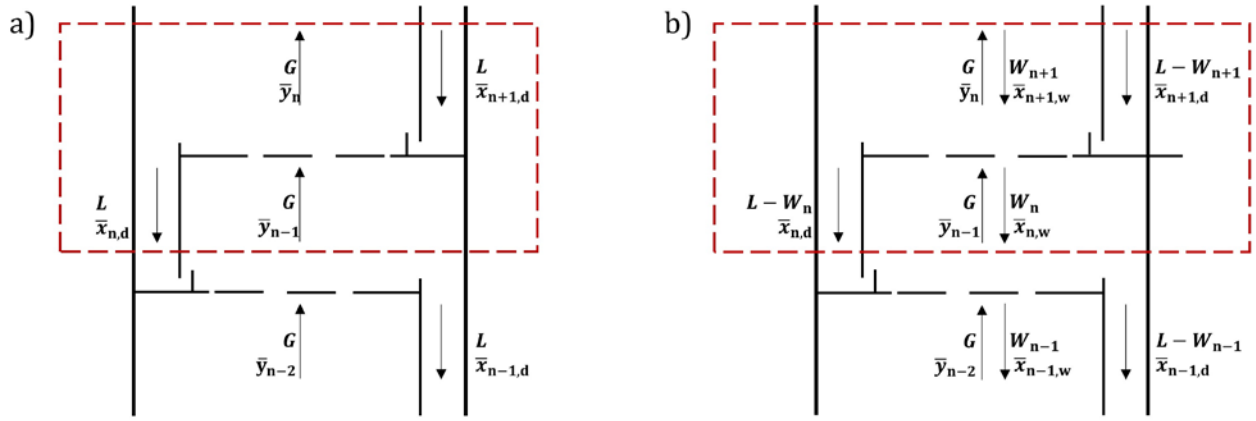

Figure 1. Nomenclature for the tray efficiency definition (highlighted by the dashed line) and for the point efficiency calculation neglecting (a) or considering weeping (b).

2.2 Vapour-side tray efficiency definition in case of weeping

In case of weeping, the concept of vapour-side tray efficiency can be adapted to account for the liquid leaving the tray via both the downcomer as well as via weeping. The definition of the so-called reduced vapour side tray efficiency was proposed by Kageyama [32] as:

$$E_{\mathrm{MV}}^{\mathrm{r}} = \frac{\bar{y}_{\mathrm{n}} - \bar{y}_{\mathrm{n-1}}}{\bar{y}_n^{\mathrm{r}*} - \bar{y}_{\mathrm{n-1}}}\,, \tag{4}$$

where

$$\bar{y}_{\mathrm{n}}^{\mathrm{r}^*} = m\bar{x}_{\mathrm{n}}^{\mathrm{r}} + b = m\left[\frac{(L - W_{\mathrm{n}})\bar{x}_{\mathrm{n,d}} + W_{\mathrm{n}}\bar{x}_{\mathrm{n,w}}}{L}\right] + b, \qquad (5)$$

$\bar{x}_{\mathrm{n,w}}$ is the average liquid concentration of the weeping liquid and W_{n} is the weeping molar flow rate from the tray (according to the nomenclature shown in **Figure 1b**).

2.3 Point efficiency

In case of perfectly mixed vapour entering the tray, the Murphree point efficiency [30] can be defined over a dispersion element as

$$E_{\mathrm{OG}} = \frac{\mathrm{y_n} - \bar{y}_{\mathrm{n-1}}}{y_{\mathrm{n}}^* - \bar{y}_{\mathrm{n-1}}}, \qquad (6)$$

where $\bar{y}_{\mathrm{n-1}}$ and y_{n} are the compositions of vapour entering and leaving the dispersion element, respectively. Here, y_{n}^* is the vapour composition that is in equilibrium with the liquid in that dispersion element.

As mentioned in Section 1, it is a common practice to determine point efficiencies of large-scale trays either based on

1) small-scale studies,
2) the estimated number of transfer units, or
3) models that relate the measured tray efficiency to the point efficiency.

The first approach assumes that the point efficiencies of large and small-scale trays are identical provided that the same physical system is used while maintaining the froth conditions. Typical experimental setups used for conducting these experiments include small cross-flow trays as well as Oldershaw columns (e.g., Manivannan et al.[24]), in which the liquid on the tray is considered as perfectly mixed, and hence, $E_{\mathrm{OG}} = E_{\mathrm{MV}}$. However, this approach does not account for wall effects that are hardly negligible at small-scale and lacks agreed criteria that allow reproducing the large-scale froth condition on a small-scale[33-34]. Proposed criteria include the fractional approach to flooding[35], the clear

liquid height and the tray geometry[36]. Other examples of small-scale studies and relevant criteria are covered by Finch and Van Winkle[37], Garrett et al.[38] and Biddulph et al.[39].

In the second approach, the number of overall gas transfer units N_{OG} is determined, which can be related to the point efficiency as

$$E_{\mathrm{OG}} = 1 - \exp(-N_{\mathrm{OG}}). \qquad (7)$$

Here, it is assumed that the gas rises in a plug flow manner, the liquid composition is vertically uniform, and the dispersion height is constant[33]. N_{OG} can be estimated using correlations derived from the experiments such as those proposed by Zuiderweg [40], Gerster et al.[41], Chan and Fair[42] and Stichlmair[43]. N_{OG} can also be estimated using semi-empirical models, which segment the overall dispersion into different regions based on their flow characteristics and predict the number of transfer units in each of those regions. An application of such models can be found in the works of Prado and Fair[16] and Syeda et al.[44]. The disadvantage of this approaches is that the applicability of the mentioned models is limited to the specific physical systems they have been developed for, while the correlations can offer reliable data only in those systems where the resistance to mass transfer is limited to the liquid side[33].

The third approach is determining the tray efficiency experimentally, and extrapolating the point efficiency according to the analytical models available in the literature. An example of this approach can be found in the study of Garcia and Fair[4]. The disadvantage of this approach is that the available models rely on assumptions (mainly on the degree of liquid mixing) that are often non-representative of the physical reality and unable to account for all the non-idealities happening on the tray. Another disadvantage is that they often require parameters (e.g., eddy diffusivity) that need additional experiments and equipment to be measured.

Only few experimental studies have been published that deal with the point efficiency measurements on large-scale setups (see **Table 1**). For example, Garcia and Fair[4], Foss et al.[14] and Prado and Fair[16] proposed experimental setups that are capable of producing perfectly-mixed froth conditions on large-scale trays, however, altering the hydrodynamics in that process. Lockett et al.[19], Lockett and Uddin[21],

Lockett and Ahmed[9] and Shore and Haselden[10] proposed the approaches based on measured liquid concentration profiles on the tray, but did not account for the transverse degree of mixing, which is a characteristic feature of large-scale trays. Lamprecht[22] measured the point efficiency at the center of the outlet weir, which cannot be considered representative of the entire tray. Thus, the present work also provides an experimental approach that allows obtaining reliable data for the point efficiency on large-scale distillation trays, accounting for both axial and transverse mixing.

3. Experimental methods and efficiency calculations

3.1 Air/water tray column mockup

The schematic diagram of the column mockup (of 800 mm ID) with design details of the tray and column is shown in **Figure 2**. The entire facility contains two sieve trays (4, 5), each with 13.55% fractional free area. The gas was supplied to the column bottom by a high-pressure blower (1) at constant temperature and humidity. To ensure a homogeneous gas distribution in the column cross-section, a baffle plate (3) was installed at the entry of the gas passage. The gas safely exits the column from the top without the need for any particular treatment. Two separate 1 m^3 tanks D1 and D2 acted as a liquid reservoir and collector, respectively. A batch of deionized water with an initial concentration of the isobutyl acetate equal to 400 ppm was prepared in advance by manually injecting (7) a known quantity of isobutyl acetate in a closed-loop circulating and mixing the liquid via centrifugal pump (P3). A mesh distributor (6) is also used to homogenize the flow of entering liquid at the column top. The liquid weeping from the lower tray was collected in a separate tank (D3) using a pump (P2). The weeping flow rate was determined by dividing the volume of liquid collected in the tank by the duration of the experiment.

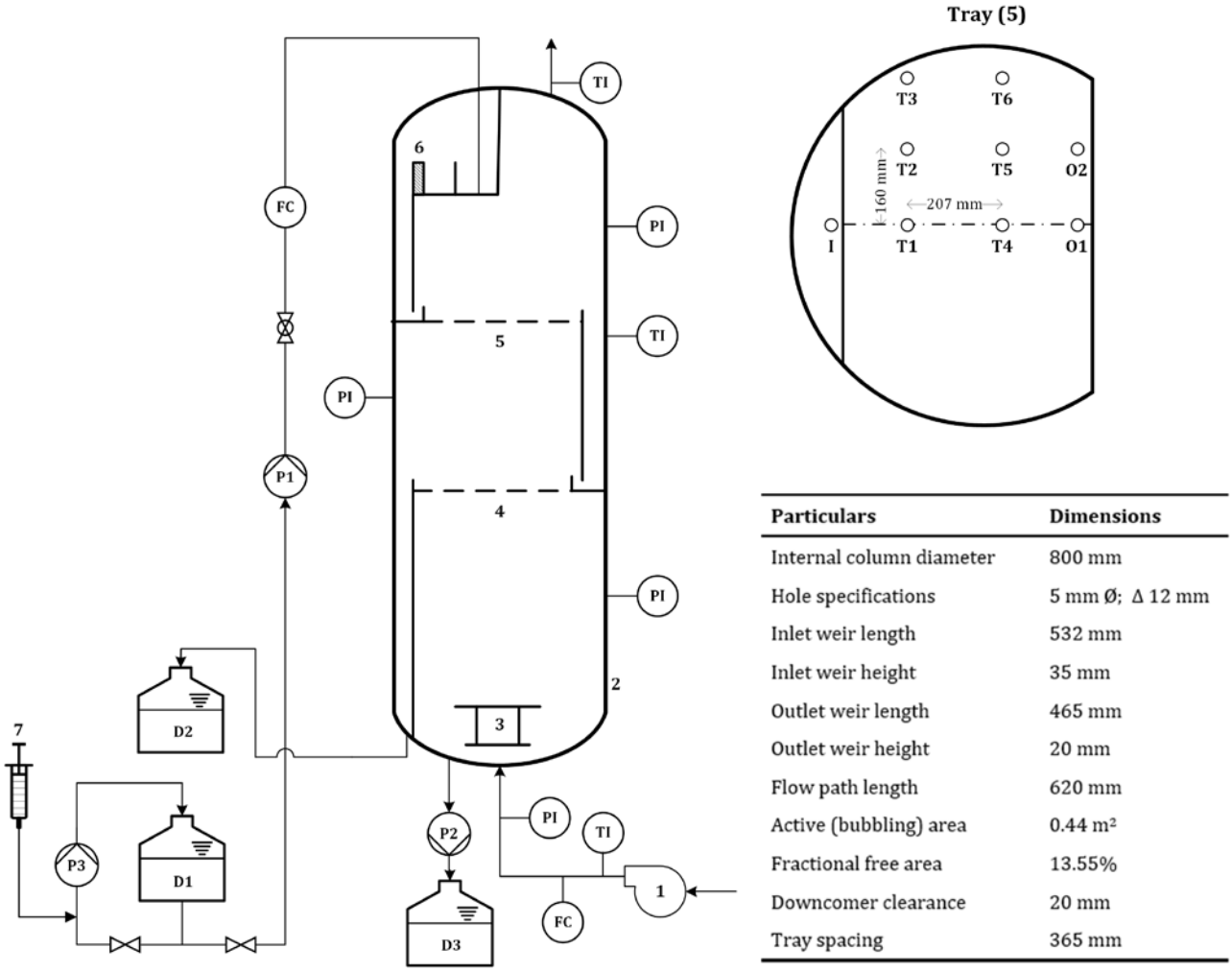

Particulars	Dimensions
Internal column diameter	800 mm
Hole specifications	5 mm Ø; Δ 12 mm
Inlet weir length	532 mm
Inlet weir height	35 mm
Outlet weir length	465 mm
Outlet weir height	20 mm
Flow path length	620 mm
Active (bubbling) area	0.44 m²
Fractional free area	13.55%
Downcomer clearance	20 mm
Tray spacing	365 mm

Figure 2. Schematics of the sieve tray column setup (D1, D2, D3 - liquid tanks, P1, P2 - liquid pumps, P3 - liquid mixing pump, TI - temperature indicator, PI - pressure indicator, FC - gas flow controller, 1- high-pressure blower, 2 - column mockup, 3 - gas inlet distributor, 4, 5 - sieve trays, 6 - liquid mesh distributor, 7 - injection system,) with dimensions and liquid sampling points.

Nine liquid sampling points were equally distributed on the tray; the location and the distance between two consecutive taps in axial and transversal direction are reported in **Figure 2** (right). The samples were collected from 20 mm high taps above the tray. Another study[45] conducted at similar tray load found that the majority of the liquid holdup is situated at around 40 mm above the tray deck. The taps with the opening at 20 mm above the deck withdrawn samples from around 40 mm height, considering pressure difference in the overall sampling line. Based on preliminary studies[45-46], the weir-to-weir liquid flow patterns on the tray can be considered as symmetric with respect to the centerline. Thus, liquid sampling from only one half of the tray is considered. Since the liquid is well-

mixed before entering the column top, only one sampling point is considered prior to the inlet weir. The liquid leaving the lower tray was also sampled before entering the outlet tank (D2).

Since the solubility of isobutyl acetate in deionized water is a function of temperature, the air was partially saturated by liquid on the lower tray acting as an air-water contactor. Such contacting prevents possible fluctuations in the liquid temperature on the test tray.

The gas and liquid loads used in the experiments are summarized in **Table 2** along with other operational parameters and the number of test repetitions performed for ensuring data reproducibility. The clear liquid height (h_{cl}) was measured using a tray-mounted U-tube manometer. The stripping factor (λ) was calculated using Henry's law as described below.

Table 2. Tray loadings and operational parameters.

f-factor ($Pa^{0.5}$)	**Weir load** ($m^3h^{-1}m^{-1}$)	**λ** (-)	h_{cl} (m)	**No. of repeats** (-)
1.77	2.15	21.5	0.009	2
1.77	4.30	11.1	0.011	2
1.77	6.45	7.2	0.012	3

3.2 Gas-liquid system and analytics

The present work introduces the air-led stripping of isobutyl acetate from aqueous solution for direct measurement of tray and point efficiencies on distillation trays. Isobutyl acetate ($C_6H_{12}O_2$) is a colorless solvent with a fruity odor and moderate solubility in water. This system was recently used for measuring liquid-side mass transfer coefficients in packed columns by Lamprecht and Burger[47], however, no previous application for distillation trays is known yet. The stripping of isobutyl acetate offers several advantages over the existing systems (see Section 1) especially for the implementation on large hydraulic installations for performance tests. In particular,

- no health and safety hazards are attributed to low concentrations of isobutyl acetate in the effluent gas stream (as prescribed by local occupational exposure limits such as TRGS 900 or the European Union Directive 2019/1831/EU), which exempts from gas treatment and recirculation duties,
- provision of a mixing pump (for batch preparation) and liquid sampling points on the tray is sufficient for efficiency tests using available air-water mockups (the system is compatible with many common installation materials such as aluminum and plastics),
- mixing of isobutyl acetate (in liquid form) with the liquid batch is much easier compared to the gas dissolution in liquid,
- liquid-side measurements can be performed using UV-spectroscopy (i.e., a fast and accepted technique for concentration measurement) without needing any gas sampling and analysis, and
- the system is applicable also for large-scale trays and even for low liquid flow rates, since the initial concentration of isobutyl acetate in the liquid batch can be adjusted according to the requirements within the safety regulations.

An initial concentration of 400 ppm isobutyl acetate in the liquid batch is selected based on preliminary tests. The physical properties of the resulting batch (i.e., viscosity, surface tension, density, etc.) remained identical to those of pure water. This permits relating the hydraulic and efficiency data obtained in the air/water column mockup. The offline UV spectrometer OceanOptics HR4000 and the OceanView 2.0 software were used for sample analysis and data acquisition, respectively. UV spectroscopy is based on the attenuation of electromagnetic radiation penetrating through a sample at a particular wavelength. According to Beer-Lambert law, the absorbance is defined as

$$A = \log_{10}\left(\frac{I_0}{I}\right), \tag{8}$$

where I and I_0 are the intensities of the attenuated and the incident radiation, respectively. Since the absorbance is related to the concentration of isobutyl acetate in the sample, the technique is suitable for quantitative analysis. All liquid samples were maintained at 17°C to minimize the effect of temperature on the absorbance value. In order to eliminate possible effects of dissolved salts on the measured absorbance and to allow a better comparison of the results from different experiments,

deionized water was used in this study. Three samples with different isobutyl acetate concentrations (100 ppm, 200 ppm and 400 ppm) were analyzed spectroscopically. The absorbance spectra at different wavelengths for each sample are plotted in **Figure 3a**. **Figure 3b** shows the linear relation between the concentration and the measured absorbance at three different wavelengths. Eventually, the 215 nm wavelength was selected to derive the linear reference relationship between the concentration of isobutyl acetate (expressed in ppm) and the absorbance as

$$C = 4815 \cdot A\,. \qquad (9)$$

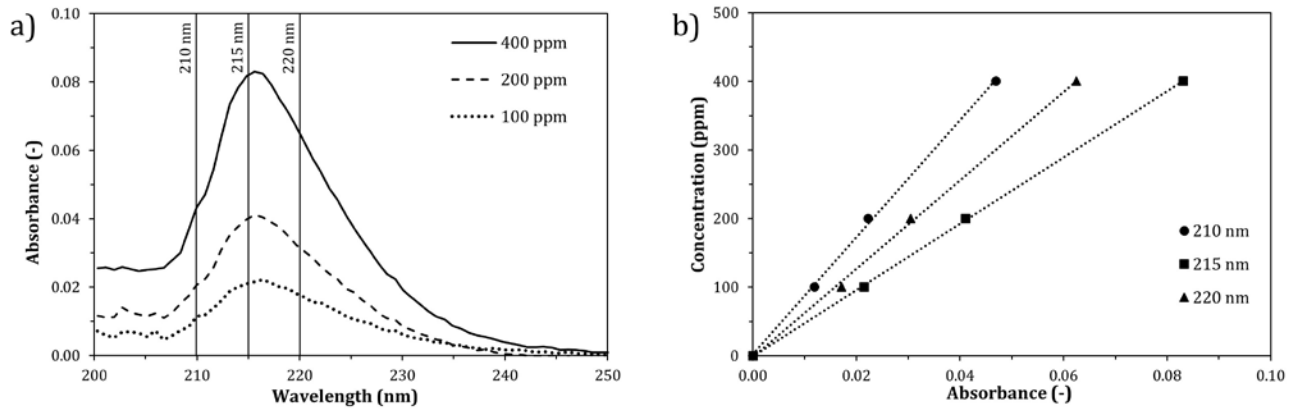

Figure 3. a) Absorbance spectrum at given wavelengths for 100 ppm, 200 ppm, and 400 ppm isobutyl acetate solution, and b) reference measurements relating solute concentration and absorbance for three different wavelengths (note that the solutions were prepared with deionized water of 9 μS/cm conductivity and the analysis was performed at 17°C).

It should be noted that the air-led stripping of isobutyl acetate from the aqueous solution is unsuitable for measuring the liquid- or gas-phase mass-transfer coefficient, because both gas- and liquid-side resistances cannot be fully neglected in the experiments. An analysis of the respective resistances is provided in Section S1 of the **Supplementary Information**. However, this did not prevent the application of the proposed method for efficiency estimation, since the determination of single-phase mass transfer coefficients was beyond the scope of this study.

It is worthwhile to mention that the influence of the hydrolysis reaction of isobutyl acetate in a dilute solution has been evaluated, which confirmed a negligible effect. The relevant assessment can be found in Section S2 of the **Supplementary Information**.

4 Efficiency calculation approaches

4.1 Point efficiency calculation neglecting weeping

Henry's law describes the equilibrium of air and an aqueous solution of isobutyl acetate according to

$$\bar{y}_{\mathrm{n}} \cdot P \cdot H^{\mathrm{cp}} = \bar{c}_{\mathrm{n}}^{*}\,, \tag{10}$$

where $\bar{c}_{\mathrm{n}}^{*}$ is the concentration of isobutyl acetate in the liquid that is in equilibrium with the vapour leaving the tray, P is the total gas pressure and H^{cp} (2.2×10^{-2} mol m^{-3}Pa^{-1}) is the Henry's constant at 25°C[48] for deionized water (as used in this study). To describe the change in solubility related to the liquid temperature T [K], Sander[48] proposed

$$\frac{d\ln(H^{\mathrm{cp}})}{d\left(\frac{1}{T}\right)} = 5500\,. \tag{11}$$

The total gas pressure was calculated via manometer-led gauge pressure of the gas entering the tray. Since the composition of the exiting vapour cannot be measured directly, a material balance was used. The approach explained in this section follows the nomenclature shown in **Figure 1a**. The overall change in vapour composition over the test tray can be written as

$$\bar{y}_{\mathrm{n}} - \bar{y}_{\mathrm{n-1}} = \frac{1}{A_{\mathrm{b}}}\int_{A_{\mathrm{b}}} (y_{\mathrm{n}} - \bar{y}_{\mathrm{n-1}})dA_{\mathrm{b}}\,, \tag{12}$$

where y_{n} is the local composition of the vapour leaving the tray n, $\bar{y}_{\mathrm{n-1}}$ is the composition of the vapour entering the tray n, that is assumed uniform (thus, $y_{\mathrm{n-1}} \equiv \bar{y}_{\mathrm{n-1}}$) and A_{b} is the tray bubbling area.

Assuming that E_{OG} is constant over the tray and using Equation 6, Equation 12 can be modified as

$$\bar{y}_{\mathrm{n}} - \bar{y}_{\mathrm{n-1}} = \frac{E_{\mathrm{OG}}}{A_{\mathrm{b}}}\int_{\mathrm{A_b}} (y_{\mathrm{n}}^{*} - \bar{y}_{\mathrm{n-1}})d\mathrm{A_b}\,. \tag{13}$$

The assumption of constant point efficiency over the tray has been widely used in the literature to simplify the tray performance assessment (e.g., Lockett and Uddin[21], Lamprecht[22]); Lockett and Dhulesia[49] also reported that the point efficiency is a week function of the superficial vapour velocity and that it can, thus, be assumed constant over the tray, regardless to any vapour maldistribution.

Using Equations 1 and 13 and considering linear vapour-liquid equilibrium, the tray-to-point efficiency ratio[41, 50] can be derived as

$$\frac{E_{\mathrm{MV}}}{E_{\mathrm{OG}}} = \frac{\frac{1}{\mathrm{A_b}}\int_{\mathrm{A_b}}(y_{\mathrm{n}}^{*} - \bar{y}_{\mathrm{n-1}})dA_b}{\bar{y}_{\mathrm{n,d}}^{*} - \bar{y}_{\mathrm{n-1}}} = \frac{\left\{\frac{1}{A_{\mathrm{b}}}\int_{A_{\mathrm{b}}}(x_{\mathrm{n}} - \bar{x}_{\mathrm{n-1}}^{*})dA_{\mathrm{b}}\right\}}{\bar{x}_{\mathrm{n,d}} - \bar{x}_{\mathrm{n-1}}^{*}}. \qquad (14)$$

Equation 14 expresses the $E_{\mathrm{MV}}/E_{\mathrm{OG}}$ ratio as a function of the liquid concentration distribution on the tray. The right term of Equation 14 contains all experimentally measured liquid concentrations apart from $\bar{x}_{\mathrm{n-1}}^{*}$, that needs to be determined considering Henry's law and the following material balance over the lower tray:

$$G(\bar{y}_{\mathrm{n-1}} - \bar{y}_{\mathrm{n-2}}) = L\left(\bar{x}_{\mathrm{n,d}} - \bar{x}_{\mathrm{n-1,d}}\right). \qquad (15)$$

The value of E_{MV} that is needed to extract E_{OG} from Equation 14 can be calculated considering Equations 2 and 3. The value of $\bar{x}_{\mathrm{n}}^{*}$, that is required in Equation 2, can be calculated considering Henry's law and the following material balance over the entire column:

$$G(\bar{y}_{\mathrm{n}} - \bar{y}_{\mathrm{n-2}}) = L(\bar{x}_{\mathrm{n+1,d}} - \bar{x}_{\mathrm{n-1,d}})\,. \qquad (16)$$

To provide a better understanding of the proposed approach, a detailed workflow is provided in Section A1 of the **Appendix**.

4.2 Efficiency calculations accounting for weeping

4.2.1 Proposed general tray and point efficiencies definitions

Hitherto, an accepted definition of the liquid-side tray efficiency at weeping conditions is missing in the literature, since the approach proposed by Kageyama[32] only provided the vapour-side tray efficiency definition. In order to provide a complete set of definitions, the following approach is proposed. The concentrations of the liquid leaving and entering the tray, $\bar{x}_{\mathrm{n,d}}$ and $\bar{x}_{\mathrm{n+1,d}}$, respectively, in Equation 2 are adjusted to account for the liquid leaving the trays via weeping. Accordingly, the generalized (reduced) liquid-side tray efficiency is

$$E_{\mathrm{ML}}^{\mathrm{r}} = \frac{\bar{x}^{\mathrm{r}}{}_{\mathrm{n+1}} - \bar{x}_{\mathrm{n}}^{\mathrm{r}}}{\bar{x}^{\mathrm{r}}{}_{\mathrm{n+1}} - \bar{x}_{\mathrm{n}}^{*}}, \tag{17}$$

where

$$\bar{x}_{\mathbf{n}}^{\mathrm{r}} = \bar{x}_{\mathrm{n,d}} - \frac{W_{\mathrm{n}}}{L}\left(\bar{x}_{\mathrm{n,d}} - \bar{x}_{\mathrm{n,w}}\right), \tag{18}$$

$$\bar{x}^{\mathrm{r}}{}_{\mathrm{n+1}} = \bar{x}_{\mathrm{n+1,d}} - \frac{W_{\mathrm{n+1}}}{L}\left(\bar{x}_{\mathrm{n+1,d}} - \bar{x}_{\mathrm{n+1,w}}\right), \text{ and} \tag{19}$$

$$\bar{y}_{\mathrm{n}} = m\bar{x}_{\mathrm{n}}^{*} + b\,. \tag{20}$$

A relationship that allows calculating the value of $E_{\mathrm{MV}}^{\mathrm{r}}$ from the measured $E_{\mathrm{ML}}^{\mathrm{r}}$ is derived in this section. Following the nomenclature in **Figure1b**, the mass balance over the n^{th} tray gives

$$(L - W_{\mathrm{n+1}})\bar{x}_{\mathrm{n+1,d}} + W_{\mathrm{n+1}}\bar{x}_{\mathrm{n+1,w}} - (L - W_{\mathrm{n}})\bar{x}_{\mathrm{n,d}} - W_{\mathrm{n}}\bar{x}_{\mathrm{n,w}} = G(\bar{y}_{\mathrm{n}} - \bar{y}_{\mathrm{n-1}}) \tag{21}$$

that can be written as

$$L(x_{\mathrm{n+1}}^{\mathrm{r}} - x_{\mathrm{n}}^{\mathrm{r}}) = G(y_{\mathrm{n}} - y_{\mathrm{n-1}}). \tag{22}$$

Considering Equations 4, 5, 17, 20 and 22,

$$\lambda = \frac{mG}{L} = \left(\frac{1}{E_{\mathrm{MV}}^{\mathrm{r}}} - 1\right) \cdot \left(\frac{1}{E_{\mathrm{ML}}^{\mathrm{r}}} - 1\right)^{-1}, \tag{23}$$

that gives

$$E_{\mathrm{MV}}^{\mathrm{r}} = \frac{E_{\mathrm{ML}}^{\mathrm{r}}}{E_{\mathrm{ML}}^{\mathrm{r}} + \lambda(1 - E_{\mathrm{ML}}^{\mathrm{r}})}, \tag{24}$$

which is the analogous relation as that of the traditional efficiency definitions (see Equation 3). Following the same path, the definition of the point efficiency can be adapted to account for weeping, too, as

$$E_{\mathrm{OG}}^{\mathrm{r}} = \frac{\mathrm{y} - \bar{y}_{\mathrm{n-1}}}{y^{\mathrm{r}^{*}} - \bar{y}_{\mathrm{n-1}}}, \tag{25}$$

where

$$y^{r^*} = mx^{r} + b\,, \tag{26}$$

where x^r is the composition of the liquid leaving the control volume accounting for weeping and defined in analogy to Equation 18. Assuming that the concentration of the liquid weeping from the control volume is the same as the liquid leaving the control volume on the tray,

$$y^{r^*} = mx^{r} + b = mx + b = y^{*}\,. \tag{27}$$

Thus, the definition of the point efficiency in the case of weeping corresponds to Equation 6.

4.2.2 Point efficiency calculation accounting for weeping

The same approach used in Section 4.1 can be applied to derive the E^{r}_{MV}/E_{OG} ratio in case of weeping according to

$$\frac{E^{r}_{MV}}{E^{r}_{OG}} = \frac{\frac{1}{A_b}\int_{A_b}(y^{*}_{n} - \bar{y}_{n-1})dA_b}{\bar{y}^{r^*}_{n} - \bar{y}_{n-1}} = \frac{\left\{\frac{1}{A_b}\int_{A_b}(x_n - \bar{x}^{*}_{n-1})dA_b\right\}}{\bar{x}^{r}_{n} - \bar{x}^{*}_{n-1}}. \tag{28}$$

The right term in Equation 28 includes x_n, which has been experimentally measured, and $\bar{x}^{r}_{\mathbf{n}}$ and $\bar{x}^{*}_{n-1}$, that have to be determined.

The definition of $\bar{x}^{r}_{n}$ was given in Equation 18 and to determine its value, W_n and $x_{n,w}$ are needed. Assuming that both trays have the same weeping rate, W_n can be taken equal to W_{n-1}, that has been measured in the experiments.

The measured liquid concentration distribution on the tray x_n and an assumed weeping distribution w_n were used to estimate the overall weeping concentration on the test tray $\bar{x}_{n,w}$. Accordingly,

$$\bar{x}_{n,w} = \frac{1}{W_n}\int_{A_b} w_n x_n dA_b\,, \tag{29}$$

where w_n is the local weeping rate per unit of the bubbling area. When selecting the weeping distribution, the following equation has to be taken into account:

$$W_{\mathrm{n}} = \int_{A_b} w_{\mathrm{n}} dA_{\mathrm{b}} \,. \tag{30}$$

In order to determine $\bar{x}^{*}_{\mathrm{n-1}}$, that is needed in Equation 28, Henry's law and the following mass balance over the lower tray should be considered:

$$G(\bar{y}_{\mathrm{n-1}} - \bar{y}_{\mathrm{n-2}}) = L(\bar{x}^{\mathrm{r}}_{\mathrm{n}} - \bar{x}^{\mathrm{r}}_{\mathrm{n-1}}) \,. \tag{31}$$

In the proposed configuration, both the total weeping rate and the average weeping concentration from the lower tray were experimentally measured. Thus, $\bar{x}^{\mathrm{r}}_{\mathrm{n-1}}$ could be directly calculated as

$$\bar{x}^{\mathrm{r}}_{\mathrm{n-1}} = \bar{x}_{\mathrm{n-1.d}} - \frac{W_{\mathrm{n-1}}}{L}\left(\bar{x}_{\mathrm{n-1,d}} - \bar{x}_{\mathrm{n-1,w}}\right) . \tag{32}$$

The value of E^{r}_{MV} that is needed to extract E^{r}_{OG} from Equation 28 can be calculated considering Equations 17 and 24. It should be noted that since in the available experimental setup no tray was located above the test tray,

$$\bar{x}^{\mathrm{r}}_{\mathrm{n+1}} = \bar{x}_{\mathrm{n+1}} \,. \tag{33}$$

The value of $\bar{x}^{*}_{\mathrm{n}}$ that is required in Equation 17, can be calculated considering Henry's law and a mass balance over the column, that gives:

$$\bar{y}_{\mathrm{n}} = \bar{\mathrm{y}}_{\mathrm{n-2}} + \frac{L(\bar{x}^{\mathrm{r}}_{\mathrm{n+1}} - \bar{x}^{\mathrm{r}}_{\mathrm{n-1}})}{G} \,. \tag{34}$$

To provide a better understanding of the proposed approach, a detailed workflow is provided in Section A2 of the **Appendix**.

5. Results and discussion

5.1 Concentration distribution and average concentration profiles

The concentration distributions were obtained by analyzing the samples along with the sampling locations on the tray. For each flow rate, the measured concentrations at the sampling points are reported in **Figure 4a-c**. **Table 3** reports the temperature of the gas leaving the tray (T_G), the gas total

pressure (P) and liquid temperature (T_L) on the test tray, the measured concentrations of the liquid leaving the downcomer of the lower tray ($\bar{C}_{n-1,d}$) and weeping from the lower tray ($\bar{C}_{n-1,w}$) and the weeping fraction. All the reported values are referred to one of the repetitions performed (see also **Table 2**); uncertainties and repeatability evaluations will be provided in Section 5.3.

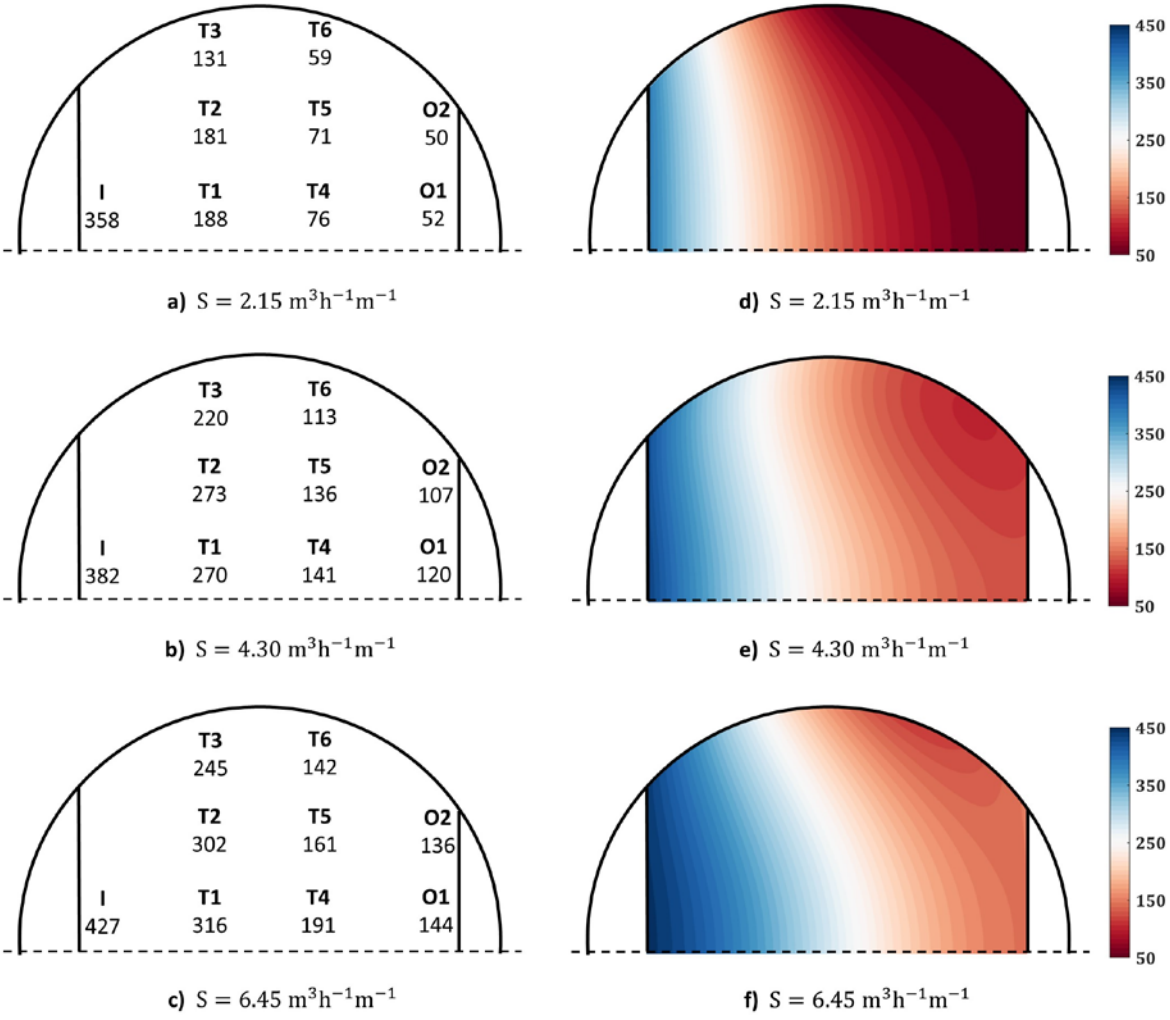

Figure 4. Liquid concentrations at sampling points (a-c) and distributed on the tray based on the polynomial fitting (d-f). Note that all concentrations are given in ppm.

Table 3. Operating conditions, outlet and weeping liquid concentration.

Weir load	T_G	P	T_L	$\bar{C}_{n-1,d}$	$\bar{C}_{n-1,w}$	**Weeping rate**
($m^3h^{-1}m^{-1}$)	(°C)	(Pa)	(°C)	(ppm)	(ppm)	($m^3h^{-1}m^{-1}$)

2.15	16	101835	13.7	8	0	0.15
4.30	16	101835	13.7	39	17	0.25
6.45	16	101835	13.7	112	52	0.47

To obtain the concentration distribution as a function of the spatial coordinates on the tray (for the sake of easier integration according to Equation 16 and 29) a polynomial fit was applied. The corresponding concentration distributions on the tray are shown in **Figure 4 (d-f).**

In **Figure 4 (a-c)**, it can be seen that at each considered flow rate, taps T1 and T2 as well as taps T4 and T5 have similar concentrations, while the concentrations at tap T3 and T6 differs from their lateral neighbors. This is compatible with a prolonged liquid residence time in the area close to the column wall possibly as a result of local recirculation zones or stagnant areas.

The weir-to-weir concentration profiles have also been evaluated taking the arithmetic averages of the respective equally-spaced taps in the direction orthogonal to the longitudinal liquid flow path. The results are shown in **Figure 5** for different weir loads (S). The concentration profile is dependent on the liquid flow rate. A lower liquid flow rate causes a higher residence time and thus, a lower outlet liquid concentration.

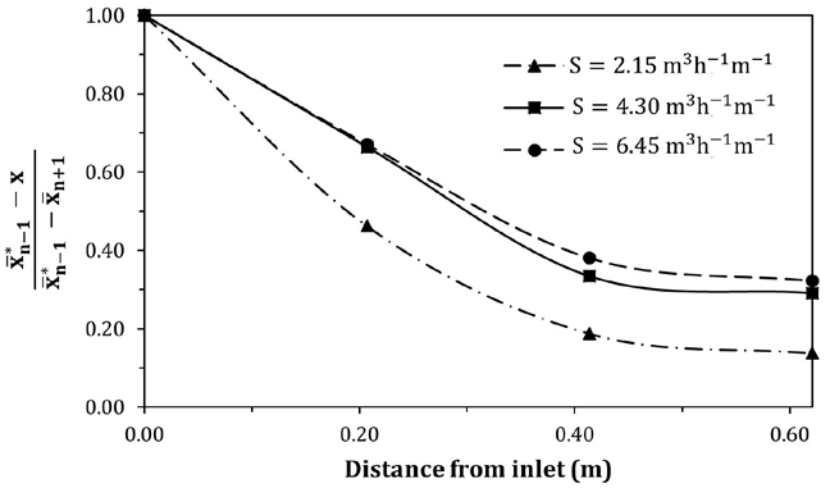

Figure 5. Liquid concentration profiles for different weir loads.

5.2 Tray and point efficiencies

5.2.1 Comparison between experimental and predicted point efficiencies

In **Figure 6**, the experimental point efficiencies obtained neglecting weeping are compared with the predictions computed using the AIChE[41] and the Zuiderweg correlations[40]. The correlations and parameters used in this section are reported in Section S3 of the **Supplementary Information**.

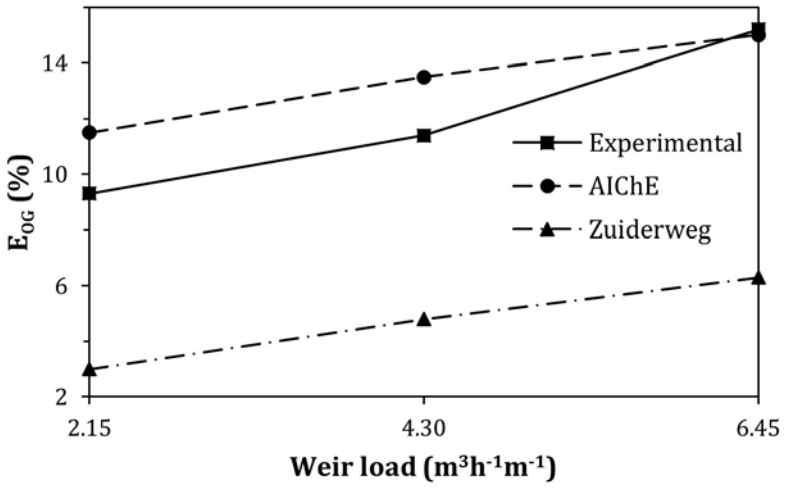

Figure 6. Experimental and predicted values for the point efficiency.

As reported by Lockett[33], the correlations give significantly different predictions. The correlation of Zuiderweg has been obtained using distillation data and is known to give a good estimate of the ratio between the gas- and liquid-side resistances, however, it does not reliably predict the absolute values of the number of transfer units (i.e., point efficiency). The AIChE correlation was developed based on stripping and absorption data. It is known to properly estimate systems with dominating liquid-side resistance and to deviate in case of systems with prevalent gas-side resistance. The good agreement between the experimental values and the AIChE model predictions is compatible with a system with prevalent resistance on the liquid side (see also the assessment provided in Section S1 of the **Supplementary Information**) and with the fact that the test system proposed here is a stripping system.

5.2.2 Comparison between experimental and predicted tray efficiencies

Figure 7 shows the comparison between the experimental tray efficiency values and the predictions using the plug-flow model (representing the upper physical limit for the tray efficiency) and the perfectly-mixed model (representing the lower physical limit for the tray efficiency) as well as the

ones obtained from the AIChE model. The mentioned efficiency models are provided in Section S3 of the **Supplementary Information**. Since these efficiency models do not account for weeping, the predicted values are compared with the experimental ones obtained by neglecting weeping, too. It should be noted that the point efficiency values predicted by the AIChE correlation and reported in **Figure 6** have been used to obtain the predictions reported in **Figure 7**.

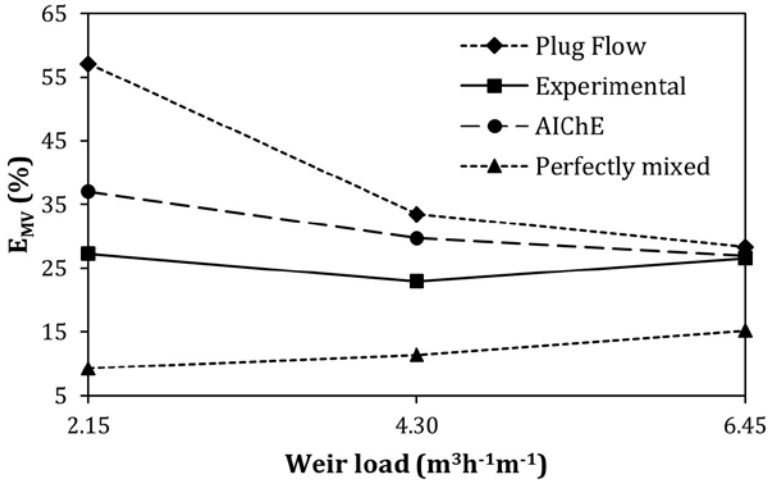

Figure 7. Experimental and predicted values for the vapour-side tray efficiency.

All experimental values of the tray efficiency (E_{MV}) are between the upper and lower physical limits. At higher weir loads, the obtained efficiency values are similar to the plug flow values, because of the minor liquid mixing happening on the tray axially. The magnitude of the experimental values is in good agreement with the predictions of the AIChE model. However, the slightly decreasing trend predicted cannot be fully reproduced by the experimental data, at least in the last data point. This inconsistency could be due to the dependency that the point efficiency value predicted by the AIChE correlation (and used to obtain the predictions shown in **Figure 7**) have on the clear liquid height. The value of the clear liquid height was determined experimentally using a tray-mounted U-tube manometer. High fluctuations in the value showed by the manometer, especially at higher liquid flow rate, have introduced an error in the measured value.

5.2.3 Effect of the liquid weeping on the measured tray and point efficiencies

In **Table 4,** the efficiency data accounting for weeping (i.e., by assuming a homogeneous weeping distribution on the upper tray) are compared with those obtained by neglecting weeping.

Table 4. Comparison between the tray and point efficiencies obtained by neglecting and considering weeping.

Weir load	E_{ML}	E_{ML}^{r}	$\frac{E_{ML} - E_{ML}^{r}}{E_{ML}}$	E_{MV}	E_{MV}^{r}	$\frac{E_{MV} - E_{MV}^{r}}{E_{MV}}$	E_{OG}	E_{OG}^{r}	$\frac{E_{OG} - E_{OG}^{r}}{E_{OG}}$
($m^3h^{-1}m^{-1}$)	(%)	(%)	(%)	(%)	(%)	(%)	(%)	(%)	(%)
2.15	89.5	85.7	4.3	26.4	20.2	23.5	9.0	8.7	3.3
4.30	77.9	73.9	5.1	22.9	19.3	15.7	11.4	10.6	7.0
6.45	73.3	69.2	5.6	25.9	22.2	14.3	14.8	14.0	5.4

As expected, the efficiencies accounting for weeping are lower than the ones obtained when weeping is neglected.

The liquid-side tray efficiency decreases with increasing liquid flow rate, which agrees well with trends reported in the literature[12-13]. It should be emphasized that the apparent inconsistency in the trend of the vapour-side tray efficiency data (i.e. partially increasing and partially decreasing) if weeping is neglected, is mitigated once weeping is considered.

The point efficiency increases with the liquid flow rates as known from the literature [51].

It should be noted that this study is not meant to evaluate the effect of weeping on tray performance, but to provide a general approach that allows determining tray and point efficiencies in case of both negligible and non-negligible weeping conditions. Since both approaches are based on the experimentally measured concentration distribution, which is the result of all the phenomena happening on the tray (e.g., channeling, recirculations, stagnant areas), including weeping, a direct comparison between the values shown in **Table 4** could be misleading. To make a meaningful evaluation, the results that account for weeping should be compared to those obtained using the concentration distribution measured at the same conditions, but without weeping. This comparison is, for clear reasons, not possible.

5.3 Repeatability and uncertainties

To test the reproducibility of the efficiency data, several repetitions of each experiment were performed (refer to Table 2). The difference in the measured absorbance values between samples taken from the same tray positions at fixed operating conditions can be mainly related to

- fluctuations of the local liquid concentration on the tray,
- the uncertainties of the UV spectrometer, and
- minor fluctuations in the sample temperature.

Considering the weir load of 6.45 $m^3h^{-1}m^{-1}$ for which the highest repetitions were performed, the recorded absorbance values differed from the average with $\pm 7\%$ variation. This is also the maximum deviation observed during the species sampling for the remaining weir loads. By assuming that the error in the measured absorbance values are randomly distributed within the given deviation, ten thousand hypothetical liquid concentration distributions were generated randomly. Efficiency calculations were performed using those distributions to quantify the uncertainty of the measured efficiency values. Weeping was neglected in this case. The probability density functions of the obtained results are illustrated in **Figure 8**.

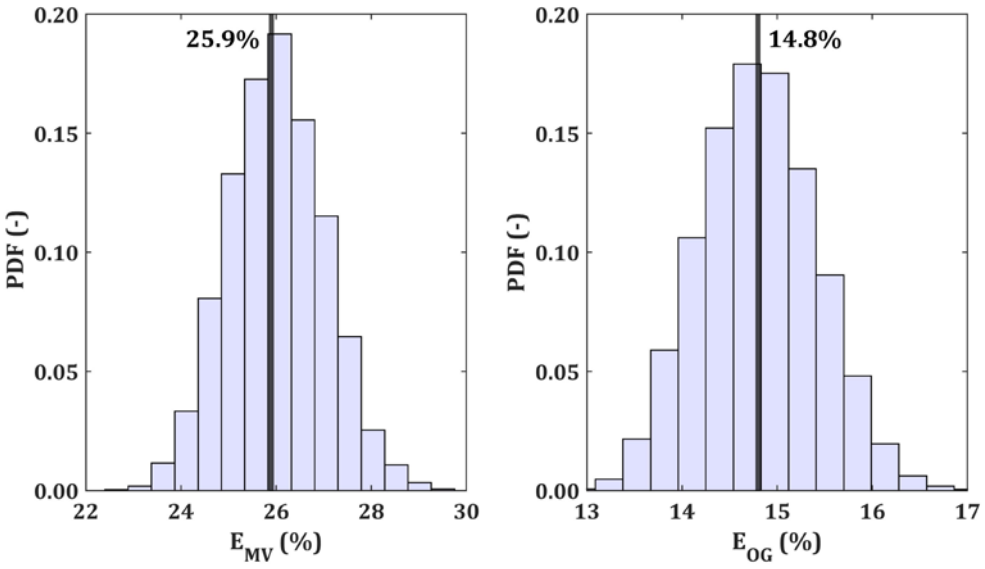

Figure 8. Probability density function (PDF) for tray (left) and point (right) efficiencies obtained from simulated concentration distributions, neglecting weeping.

The resulting standard deviation is 0.6% for the point efficiency and 1.0% for the tray efficiency.

6. Conclusion and further developments

The stripping of isobutyl acetate from an aqueous solution using air is a very promising candidate for investigating tray and point efficiencies of distillation trays. The use of this system allows overcoming the main criticisms related to traditional systems. No significant hazards are related to the use of the substance at low concentrations and no up- and downstream treatment on the gas stream is required. The preparation of the initial solution can easily be done since isobutyl acetate is a liquid at ambient conditions. The possibility of increasing the initial concentration of isobutyl acetate allows applying the system to large trays also at low liquid flow rates. The proposed experimental setup is relatively easy to implement in existing cold fluid air/water mockups designed for hydrodynamic studies. Since the addition of small quantities of isobutyl acetate does not affect the liquid properties, the measured efficiency values can be combined with hydrodynamic data obtained with air/water systems.

This work is one of the few examples in the literature, in which the experimental determination of the point efficiency in a large-scale distillation tray is attempted and achieved. Since the determined values of the point efficiency are based on the actual liquid concentration distribution on the tray, it also takes into account axial and transversal liquid mixing, stagnant areas, recirculation, channeling and other possible flow non-idealities.

A full set of definitions for tray and point efficiencies in case of weeping has been provided in this work and the proposed approach was shown to be applicable for investigating the effect of tray and point efficiency at weeping conditions.

The measured tray and point efficiency values (also accounting for the effect of weeping) can be used to validate tray efficiency models. The proposed method is also suitable for evaluating the performance of devices (such as flow conditioners) used to improve the tray design and to prevent stagnant areas and to provide experimental validation benchmarks for CFD distillation tray models.

Acknowledgment

S. M. acknowledges the financial support of the Erasmus+ program of the European Union. V. V. acknowledges the financial support from the German Academic Exchange Service (Deutscher Akademischer Austauschdienst, DAAD, grant number: 91563198).

Supporting Information

This information is available free of charge via the Internet at http://pubs.acs.org/.

Nomenclature

Symbol	Description	Unit
$\boldsymbol{A}$	Absorbance	
$\boldsymbol{A_b}$	Tray bubbling area	m^2
$\boldsymbol{b}$	Intercept of the linearized vapour-liquid equilibrium data	
$\boldsymbol{c}$	Liquid concentration	mol m^{-3}
$\boldsymbol{c^*}$	Liquid equilibrium concentration	mol m^{-3}
$\boldsymbol{C}$	Liquid concentration	ppm
$\boldsymbol{E_{MV}}$	Murphree vapour-side tray efficiency	
$\boldsymbol{E_{ML}}$	Murphree liquid-side tray efficiency	
$\boldsymbol{E_{OG}}$	Murphree vapour-side point efficiency	
$\boldsymbol{G}$	Molar vapour flow rate	mol s^{-1}
$\boldsymbol{H^{cp}}$	Henry constant	mol $m^{-3}Pa^{-1}$
$\boldsymbol{h_{cl}}$	Clear liquid height	m
I	Transmitted UV radiation intensity	W
$\boldsymbol{I_0}$	Incident UV radiation intensity	W
$\boldsymbol{L}$	Molar liquid flow rate	mol s^{-1}
$\boldsymbol{m}$	Slope of the linearized vapour-liquid equilibrium data	

$\boldsymbol{N_{OG}}$	Number of overall gas transfer units	
$\boldsymbol{P}$	Pressure	Pa
S	Weir load	$m^3h^{-1}m^{-1}$
$\boldsymbol{T}$	Temperature	K
$\boldsymbol{x}$	Local liquid molar fraction	
$\boldsymbol{\bar{x}}$	Average liquid molar fraction	
$\boldsymbol{\bar{x}^*}$	Liquid equilibrium molar fraction	
$\boldsymbol{y}$	Local vapour molar fraction	
$\boldsymbol{\bar{y}}$	Average vapour molar fraction	
$\boldsymbol{y^*}$	Local vapour equilibrium molar fraction	
$\boldsymbol{\bar{y}^*}$	Vapour equilibrium molar fraction	
$\boldsymbol{L_w}$	Outlet weir length	m
$\boldsymbol{\lambda}$	Stripping factor	

Subscripts

$\boldsymbol{G}$	Gas
$\boldsymbol{L}$	Liquid
$\boldsymbol{n}$	Tray number
$\boldsymbol{d}$	Downcomer
$\boldsymbol{w}$	Weeping

References

1. Gorak, A.; Sorensen, E. *Distillation: fundamentals and principles*. Elsevier Science: Burlington, VT, 2014.
2. Glüera, S.; Gäblera, A.; Angb, C., Limitations of Air/Water Testing in the Development of High Performance Trays. *Chem. Eng. Trans.* **2018,** *69*, 805-810.

3. Yanagi, T.; Sakata, M., Performance of a commercial scale 14% hole area sieve tray. *Ind. Eng. Chem. Process Des. Dev.* **1982,** *21* (4), 712-717.
4. Garcia, J. A.; Fair, J. R., A fundamental model for the prediction of distillation sieve tray efficiency. 1. Database development. *Ind. Eng. Chem. Res.* **2000,** *39* (6), 1809-1817.
5. Mayfield, F. D.; Church, W. L.; Green, A. C.; Lee, D. C.; Rasmussen, R. W., Perforated-plate distillation columns. *Ind. Eng. Chem.* **1952,** *44* (9), 2238-2249.
6. Jones, J. B.; Pyle, C., Relative performance of sieve and bubble-cap plates. *Chem. Eng. Prog.* **1955,** *51* (9), 424-427.
7. Rush Jr, F. E.; Stirba, C., Measured plate efficiencies and values predicted from single-phase studies. *AIChE J.* **1957,** *3* (3), 336-342.
8. Kaŝtánek, F.; Standart, G., Studies on Distillation: XX. Efficiency of Selected Types of Large Distillation Trays at Total Reflux. *Sep. Sci. Technol.* **1967,** *2* (4), 439-486.
9. Lockett, M.; Ahmed, I., Tray and point efficiencies from a 0.6 metre diameter distillation column. *Chem. Eng. Res. Des.* **1983,** *61* (2), 110-118.
10. Shore, D.; Haselden, G. G., Liquid mixing on distillation plates and its effect on plate efficiency. *Inst. Chem. Eng. Symp. Ser.* **1969,** *32*, 2:54.
11. Anderson, R. H.; Garrett, G.; Vanwinkle, M., Efficiency Comparison of Valve and Sieve Trays in Distillation Columns. *Ind. Eng. Chem. Process Des. Dev.* **1976,** *15* (1), 96-100.
12. Thomas, W. J.; Haq, M. A., Studies of the performance of a sieve tray with 3/8-in. diameter perforations. *Ind. Eng. Chem. Process Des. Dev.* **1976,** *15* (4), 509-518.
13. AIChE *Bubble-tray design manual prediction of fractionation efficiency*. AIChE: New York, NY, 1958.
14. Foss, A. S.; Gerster, J. A.; Pigford, R. L., Effect of Liquid Mixing on the Performance of Bubble Trays. *AIChE J.* **1958,** *4*, 231-239.
15. Sun, Z.; Liu, C.; Yu, G.; Yuan, X., Prediction of distillation column performance by computational mass transfer method. *Chin. J. Chem. Eng.* **2011,** *19* (5), 833-844.
16. Prado, M.; Fair, J. R., Fundamental model for the prediction of sieve tray efficiency. *Ind. Eng. Chem. Res.* **1990,** *29* (6), 1031-1042.
17. Nutter, D. E., Ammonia Stripping Efficiency Study *AlChE Symp. Ser.* **1971,** *68* (124), 73-83.
18. Johnson, A.; Marangozis, J., Mixing studies on a perforated distillation plate. *Can. J. Chem. Eng.* **1958,** *36* (4), 161-168.
19. Lockett, M. J.; Kirkpatrick, R. D.; Uddin, M. S., Froth regime point efficiency for gas/film controlled mass transfer on a two-dimensional sieve tray. *Trans IChemE* **1979,** *57*, 25-34.
20. Thomas, W. J.; Ogboja, O., Mass transfer studies on sieve trays with 1-in. diameter perforations. *Ind. Eng. Chem. Process Des. Dev.* **1982,** *21* (2), 217-222.
21. Lockett, M. J.; Uddin, M. S., Liquid-phase controlled mass transfer in froths on sieve trays. *Trans IChemE* **1980,** *58*, 166-174.

22. Lamprecht, J. H. The development of simplistic and cost-effective methods for the evaluation of tray and packed column efficiencies. M.S. Thesis, Stellenbosch University, Republic of South Africa, 2017.
23. Budavari, S. *The Merck Index: An Encyclopedia of Chemicals, Drugs, and Biologicals*. 12th ed.; Merck & Co.: Whitehouse station, NJ, 1996.
24. Manivannan, R. G.; Cai, T.; McCarley, K.; Vennavelli, A.; Aichele, C. P., Evaluation of the validity of tray and point efficiency correlations at elevated liquid viscosities and proposal of an improved point efficiency correlation. *Chem. Eng. Res. Des.* **2020,** *159*, 27-35.
25. Smith, V. C.; Upchurch, J. C.; Weiler, D. W., Advantages of small hole sieve trays in a water scrubber. *Chem. Eng. Progress* **1981,** *77* (9), 48-54.
26. Raju, K. *Fluid mechanics, heat transfer, and mass transfer: chemical engineering practice*. Wiley: Hoboken, NJ, 2011.
27. Lockett, M.; Rahman, M.; Dhulesia, H., Prediction of the effect of weeping on distillation tray efficiency. *AIChE J.* **1984,** *30* (3), 423-431.
28. Banik, S. Weeping from distillation trays. Ph.D. Dissertation, University of Manchester, U.K., 1982.
29. Billingham, J.; Banik, S.; Lockett, M., The effect of inlet weeping on distillation tray efficiency. *Chem. Eng. Res. Des.* **1995,** *73* (4), 385-391.
30. Murphree, E. V., Rectifying Column Calculations. *Ind. Eng. Chem.* **1925,** *17* (7), 747-750.
31. Taylor, R.; Duss, M., 110th Anniversary: Column Efficiency: From Conception, through Complexity, to Simplicity. *Ind. Eng. Chem. Res.* **2019,** *58* (36), 16877-16893.
32. Kageyama, O., Plate efficiency in distillation towers with weeping and entrainment. *Inst. Chem. Eng. Symp. Ser.* **1969,** *32*, 2:72.
33. Lockett, M. J. *Distillation tray fundamentals*. Cambridge University Press: Cambridge, NY, 1986.
34. Foss, A. S. Liquid mixing on bubble trays and its effect upon plate efficiency. Ph.D. Dissertation, University of Delaware, Nawark, DE, 1957.
35. Fair, J. R.; Null, H. R.; Bolles, W. L., Scale-up of plate efficiency from laboratory Oldershaw data. *Ind. Eng. Chem. Process Des. Dev.* **1983,** *22* (1), 53-58.
36. Lopez, F.; Castells, F., Influence of tray geometry on scaling up distillation efficiency from laboratory data. *Ind. Eng. Chem. Res.* **1999,** *38* (7), 2747-2753.
37. Finch, R.; Van Winkle, M., A statistical correlation of the efficiency of perforated trays. *Ind. Eng. Chem. Process Des. Dev.* **1964,** *3* (2), 106-116.
38. Garrett, G. R.; Anderson, R. H.; Van Winkle, M., Calculation of Sieve and Valve Tray Efficiencies in Column Scale-up. *Ind. Eng. Chem. Process Des. Dev.* **1977,** *16* (1), 79-82.
39. Biddulph, M. W.; Rocha, J. A.; Bravo, J. L.; Fair, J. R., Point efficiencies on sieve trays. *AIChE J.* **1991,** *37* (8), 1261-1264.

40. Zuiderweg, F. J., Sieve trays: a view on the state of the art. *Chem. Eng. Sci.* **1982,** *37* (10), 1441-1464.
41. Gerster, J. A.; Hill, A. B.; Hochgraf, N. N.; Robinson, D. G. *Tray Efficiencies in Distillation Columns: Final Report from the University of Dalaware*. AIChE: New York, NY, 1958.
42. Chan, H.; Fair, J. R., Prediction of point efficiencies on sieve trays. 1. Binary systems. *Ind. Eng. Chem. Process Des. Dev.* **1984,** *23* (4), 814-819.
43. Stichlmair, J., Grundlagen der Dimensionierung des Gas/Flüssigkeit-Kontaktapparates Bodenkolonne. *Chem. Ing. Tech.* **1978,** *50* (4), 281-284.
44. Syeda, S. R.; Afacan, A.; Chuang, K. T., A fundamental model for prediction of sieve tray efficiency. *Chem. Eng. Res. Des.* **2007,** *85* (2), 269-277.
45. Vishwakarma, V.; Schleicher, E.; Bieberle, A.; Schubert, M.; Hampel, U., Advanced flow profiler for two-phase flow imaging on distillation trays. *Chem. Eng. Sci.* **2021,** *231*, 116280 ff.
46. Schubert, M.; Piechotta, M.; Beyer, M.; Schleicher, E.; Hampel, U.; Paschold, J., An imaging technique for characterization of fluid flow pattern on industrial-scale column sieve trays. *Chem. Eng. Res. Des.* **2016,** *111*, 138-146.
47. Lamprecht, J. H.; Burger, A. J., Desorption of Isobutyl Acetate into Air as a Low-Cost Alternative System for the Measurement of Liquid Phase Mass Transfer Coefficients. *Chem. Eng. Trans.* **2018,** *69*, 7-12.
48. Sander, R., Compilation of Henry's law constants (version 4.0) for water as solvent. *Atmos. Chem. Phys.* **2015,** *15* (8), 4399-4981.
49. Lockett, M.; Dhulesia, H., Murphree plate efficiency with nonuniform vapour distribution. *Chem. Eng. J.* **1980,** *19* (3), 183-188.
50. Vishwakarma, V.; Schubert, M.; Hampel, U., Assessment of separation efficiency modeling and visualization approaches pertaining to flow and mixing patterns on distillation trays. *Chem. Eng. Sci.* **2018,** *185*, 182-208.
51. Wijn, E., Does the Point Efficiency on Sieve Trays Depend on Liquid Height and Flow Regime? *Chem. Eng. Sym. Ser.* **1997,** *142*, 809-816.

Appendix

A1. Efficiency calculation procedure neglecting weeping

The following points summarize the calculation procedure for point efficiency in case weeping is neglected:

1. From the experiments the following parameters are known: $\bar{x}_{\mathrm{n+1,d}}, x_{\mathrm{n}}, \bar{x}_{\mathrm{n,d}}, \bar{x}_{\mathrm{n-1,d}}, \bar{x}_{\mathrm{n-1,w}}, W_{\mathrm{n-1}}, L, \bar{y}_{\mathrm{n-2}}\ G, P,\ T_{\mathrm{L}}$
2. Calculate $\bar{y}_{\mathrm{n}}$ using Equation 16
3. Calculate the value of H^{cp} at T_{L} using Equation 11
4. Calculate $\bar{c}^{*}_{\mathrm{n}}$ using Equation 10 and convert this concentration value into molar fraction ($\bar{x}^{*}_{\mathrm{n}}$)
5. Calculate the liquid-side tray efficiency using Equation 2
6. Calculate λ
7. Calculate the vapour-side tray efficiency using Equation 3
8. Calculate $\bar{y}_{\mathrm{n-1}}$ using Equation 15
9. Calculate $\bar{c}^{*}_{\mathrm{n-1}}$ using Equation 10 and convert this concentration value into molar fraction ($\bar{x}^{*}_{\mathrm{n-1}}$)
10. Calculate the vapour-side point efficiency using Equation 14

A2. Efficiency calculation procedure considering weeping

The following points summarize the calculation procedure for point efficiency in case weeping is considered:

1. From the experiments, the following parameters are known: $x_{\mathrm{n+1,d}}, x_{\mathrm{n}}, x_{\mathrm{n,d}}, x_{\mathrm{n-1,d}}, x_{\mathrm{n-1,w}}, W_{\mathrm{n-1}}, L, \bar{y}_{\mathrm{n-2}},\ G, P,\ T_{\mathrm{L}}$
2. Calculate $\bar{x}^{r}_{\mathrm{n+1}}$ using Equation 19
3. Calculate $\bar{x}^{r}_{\mathrm{n-1}}$ using Equation 33

4. Calculate $\bar{y}_{\mathrm{n}}$ using Equation 34
5. Calculate the value of H^{cp} at T_{L} using Equation 11
6. Calculate $\bar{c}_{\mathrm{n}}^{*}$ using Equation 10 and convert this concentration value into molar fraction ($\bar{x}_{\mathrm{n}}^{*}$)
7. If not experimentally available, assume a weeping distribution considering Equation 30 and calculate $\bar{x}_{\mathrm{n,w}}$ using Equation 29
8. Calculate $\bar{x}_{\mathrm{n}}^{r}$ using Equation 18
9. Calculate the liquid-side tray efficiency using Equation 17
10. Calculate λ
11. Calculate the vapour-side tray efficiency using Equation 24
12. Calculate $\bar{y}_{\mathrm{n}-1}$ using Equation 32
13. Calculate $\bar{c}_{\mathrm{n}-1}^{*}$ using Equation 10 and convert this concentration value into molar fraction ($\bar{x}_{\mathrm{n}-1}^{*}$)
14. Calculate the vapour-side point efficiency using Equation 28

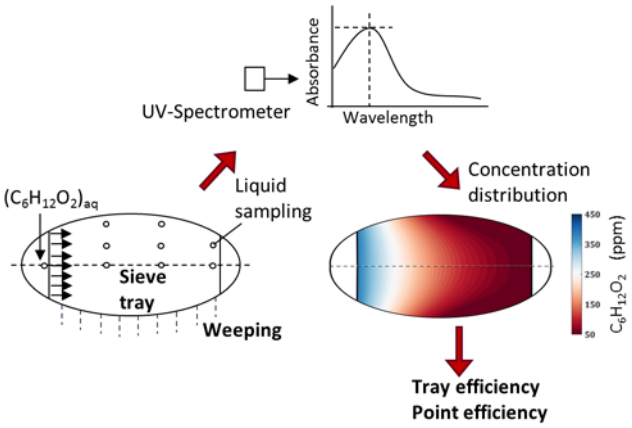

For Table of Contents Only